

Fast Radio Bursts as probes of the late-time universe: a new insight on the Hubble tension

Surajit Kalita^{1,*}, Shruti Bhatporia^{1,†} and Amanda Weltman^{1,2,‡}

¹*High Energy Physics, Cosmology and Astrophysics Theory (HEPCAT) Group,
Department of Mathematics and Applied Mathematics,
University of Cape Town, Cape Town 7700, South Africa*

²*African Institute for Mathematical Sciences, 6 Melrose Road, Muizenberg 7945, South Africa*

Fast Radio Bursts (FRBs) are bright radio transient events, a subset of which have been localized to their host galaxies. Their high dispersion measures offer valuable insights into the ionized plasma along their line of sight, enabling them to serve as probes of cosmological parameters. One of the major challenges in contemporary cosmology is the Hubble tension – an unresolved discrepancy between two independent methods of determining the Universe’s expansion rate, yielding differing values for the Hubble constant. In this study, we analyze a sample of 64 extragalactic, localized FRBs observed by various telescopes, employing Bayesian analysis with distinct likelihood functions. Our findings suggest that FRBs serve as tracers of the Hubble constant in the late-time Universe. Notably, our results exhibit smaller error bars compared to previous studies, and the derived Hubble constant with 1σ error bars no longer overlap with those obtained from early-Universe measurements. These results underscore the continuing tension between early- and late-time measurements of the Hubble constant.

1. INTRODUCTION

Fast Radio Bursts (FRBs) are short-lived yet exceptionally energetic radio wave transients originating from mostly extragalactic sources. First reported in 2007 [1], FRBs remain an enigmatic phenomenon in astrophysics. These bursts typically persist for only milliseconds, but can release immense energy, exhibiting peak flux densities on the order of several Janskys. All observed FRBs span a radio frequency range of roughly 100 MHz to 8 GHz [2, 3]. High dispersion measures (DMs) associated with FRBs, a measure of the electron density along the line of sight, offer insights into the intervening medium and thus their distances. These DMs strongly suggest an extragalactic origin for most FRBs. A singular, notable exception exists: FRB 20200428A, confirmed to have originated from the Galactic magnetar SGR 1935+2154 [4–6]. Although the intervening interstellar and intergalactic medium (IGM), in general, introduces uncertainties in these distance estimates, several FRBs have been localized to host galaxies. For instance, the repeating FRB 20121102A was traced to a dwarf galaxy at a luminosity distance of 972 Mpc [7].

Over 700 FRBs have been detected to date, with the majority identified through the Canadian Hydrogen Intensity Mapping Experiment (CHIME) radio telescope¹. However, there is a growing number of events from other radio observatories, such as the Australian Square Kilometre Array Pathfinder (ASKAP)² and MeerKAT³, re-

flecting a rapid increase in discovery rates. Most FRBs are detected as singular, non-repeating events, with no apparent recurrence from the same source. Nevertheless, a small subset of FRBs exhibit repeating behavior, with repeated bursts originating from a consistent location, facilitating in-depth source characterization. FRB 20121102A is a well-known example of a repeating FRB, with over hundred bursts observed to date. The variability in repetition rates across observed FRBs suggests multiple potential astrophysical origins or mechanisms, posing challenges for a unified theoretical framework. Studying FRBs provides crucial insights into high-energy astrophysical processes and the extreme environments surrounding compact objects such as neutron stars and black holes.

Despite significant progress, the exact origins of FRBs remain uncertain, although several hypotheses have been advanced. The hypothesis of a magnetar origin has garnered substantial support [8], yet unresolved questions remain, as magnetars are not proven to take into account for all observed FRB phenomena. Notably, only one FRB has been definitively linked to a Galactic magnetar. Consequently, alternative theories are being considered, with some models proposing connections to black holes or white dwarfs. For comprehensive reviews on potential progenitor mechanisms, see [9] and [10]. Future multi-messenger observations, incorporating gravitational wave (GW) and neutrino detections associated with FRB sources, offer promising avenues for uncovering the astrophysical processes responsible for FRBs [11].

FRBs, traveling across significant cosmological distances, provide a valuable tool for probing the IGM, including the distribution of matter within it. Their unique characteristics, such as short pulse durations, high DMs, and the ability to probe the IGM on cosmological scales, make them effective in addressing various astrophysical and cosmological questions. For instance,

* E-mail: surajit.kalita@uct.ac.za

† E-mail: shrutibhatporia@gmail.com

‡ E-mail: amanda.weltman@uct.ac.za

¹ <https://chime-experiment.ca/en>

² <https://www.atnf.csiro.au/projects/askap/index.html>

³ <https://www.sarao.ac.za/science/meerkat/>

FRB 20150418A has been used to place constraints on the photon mass, limiting it to $m_\gamma < 1.8 \times 10^{-14} \text{ eV c}^{-2}$ [12]. Subsequent studies of multiple FRBs have strengthened this constraint [13, 14]. In addition, the application of gravitational lensing to FRBs has allowed for constraints on the fraction of dark matter that may consist of primordial black holes [15–20]. Moreover, by marginalizing over the contributions from both the host galaxy and free electrons in 12 FRBs, constraints were put on the parameterized post-Newtonian parameter to test the weak equivalence principle and found that it is consistent with unity within 1 part in 10^{13} at the 68% confidence level [21], representing one of the tightest bounds in this low-energy regime. Recently, localized FRBs have also been utilized to constrain additional fundamental constants, such as the fine-structure constant and the proton-to-electron mass ratio [22, 23].

Several recent studies have utilized FRBs with measured redshifts to constrain the Hubble constant (H_0), primarily leveraging Bayesian analysis techniques. Walters et al. [24] pioneered the exploration of FRBs as cosmological probes by employing mock FRB catalogs, illustrating the potential for significant enhancements in the precision of cosmological parameter constraints when combined with data from the cosmic microwave background (CMB), baryonic acoustic oscillations (BAOs), supernovae, and H_0 measurements. Macquart et al. [25] used eight localized FRBs to constrain the baryonic matter density $\Omega_b = 0.051_{-0.025}^{+0.021} h_{70}^{-1}$, where $h_{70} = H_0 / (70 \text{ km s}^{-1} \text{ Mpc}^{-1})$, consistent with prior estimates derived from CMB and Big Bang nucleosynthesis data. Additionally, a study employing strong lensing effects from 10 FRBs reported a value of $H_0 \approx 70 \text{ km s}^{-1} \text{ Mpc}^{-1}$ [26].

With the increasing number of localized FRBs, these constraints have undergone substantial refinements. Hagstotz et al. [27] analyzed nine localized FRBs, estimating $H_0 = 62.3 \pm 9.1 \text{ km s}^{-1} \text{ Mpc}^{-1}$, assuming a homogeneous contribution from the host galaxy, a factor that may limit the robustness of this estimate. Subsequently, Wu et al. [28] classified 18 localized FRBs based on host galaxy morphology employing the IllustrisTNG simulation, to estimate individual host contributions, leading to an estimate of $H_0 = 68.81_{-4.33}^{+4.99} \text{ km s}^{-1} \text{ Mpc}^{-1}$. However, the host DM values predicted by their model were found to be lower than the observed values for some FRBs. Furthermore, James et al. [29] included 16 localized and 60 unlocalized FRBs detected by ASKAP, obtaining $H_0 = 73_{-8}^{+12} \text{ km s}^{-1} \text{ Mpc}^{-1}$. The larger uncertainty in their result, despite the larger sample size, likely reflects the inclusion of systematic uncertainties. Subsequent research has investigated a variety of statistical methods, simulations, and FRB datasets to further constrain H_0 [30–34]. More recently, Fortunato et al. [35] proposed a novel approach using artificial neural networks with 23 localized FRBs, yielding an estimate of $H_0 = (67.3 \pm 6.6) \text{ km s}^{-1} \text{ Mpc}^{-1}$.

Although FRBs provide valuable preliminary con-

straints on cosmological parameters, we do not yet have enough observations with localizations to resolve the ongoing tensions in cosmology. While less stringent than those obtained from CMB and Type Ia supernovae (SNeIa) data, the constraints derived from FRBs are tighter than those obtained from GW observations. The discrepancies in the reported values of H_0 primarily arise from uncertainties in modeling the contributions from the IGM and the host galaxy’s DM. In this study, we apply various statistical methodologies to a comprehensive dataset of 64 localized, extragalactic FRBs to derive new constraints on H_0 . Our analysis reveals substantial improvements in uncertainty compared to previous studies and shows consistency with recent late-time Universe measurements from the SH0ES collaboration [36]. These findings provide a significant contribution towards highlighting the tension between early- and late-time Universe H_0 estimates.

This article is structured as follows. In Section 2, we revisit the key relationships between the DM and host redshift, and their dependencies on H_0 . Section 3 describes our data sample, consisting of 64 localized FRBs, which is subsequently used to estimate H_0 through a Bayesian analysis. We employ three distinct methods with different likelihood functions to calculate H_0 , accounting for the various uncertainties in the DM components of FRBs. Section 4 provides a detailed discussion of the results showing our results are in alignment with the late-time Universe measurements of H_0 . Finally, our conclusions are presented in Section 5.

2. REVISITING DISPERSION MEASURE OF FAST RADIO BURSTS

A key feature exhibited by FRBs is the dispersion sweep observable in the frequency-time domain. This effect arises from the presence of the ionized plasma along the line of sight of the radio waves from the source to the telescope. The degree of dispersion is characterized by DM, which quantifies the total column density of free electrons encountered by the signal. The DM is primarily composed of contributions from four distinct regions: the Milky Way Galaxy (DM_{MW}), its circumgalactic halo (DM_{Halo}), the IGM (DM_{IGM}), and the host galaxy of the FRB (DM_{Host}). Denoting the source redshift as z_S , the total DM contributions can be expressed as

$$\text{DM} = \text{DM}_{\text{MW}} + \text{DM}_{\text{Halo}} + \text{DM}_{\text{IGM}}(z_S) + \frac{\text{DM}_{\text{Host}}}{1 + z_S}. \quad (1)$$

Given our well-established understanding of the Galactic distribution of free electrons, the Milky Way’s DM DM_{MW} is modeled with reasonable accuracy. Additionally, it was already estimated that the Galactic halo contributes approximately $\text{DM}_{\text{Halo}} \approx 50 - 80 \text{ pc cm}^{-3}$, independent of the contribution from the Galactic interstellar medium [37]. The remaining components, specifically DM_{IGM} and DM_{Host} remain less well constrained

due to the challenges inherent in their measurements. However, simulations from IllustrisTNG suggest that for non-repeating FRBs, the median host galaxy contribution is $DM_{\text{Host}} = 33(1 + z_S)^{0.84} \text{ pc cm}^{-3}$, whereas for repeating FRBs, it varies between $35(1 + z_S)^{1.08} \text{ pc cm}^{-3}$ for dwarf galaxies and $96(1 + z_S)^{0.83} \text{ pc cm}^{-3}$ for spiral galaxies [38].

The average DM_{IGM} , known as the Macquart relation, is expressed as [25]

$$\langle DM_{\text{IGM}}(z_S) \rangle = \frac{3c\Omega_b H_0^2}{8\pi G m_p} \int_0^{z_S} \frac{f_{\text{IGM}}(z)\chi(z)(1+z)}{H(z)} dz, \quad (2)$$

where c represents the speed of light, G is the gravitational constant, m_p is the proton mass, f_{IGM} is the baryon fraction in the IGM, and $\chi(z)$ is the ionization fraction along the line of sight. The ionization fraction $\chi(z)$ is given by

$$\chi(z) = Y_{\text{H}}\chi_{\text{e,H}}(z) + \frac{1}{2}Y_{\text{p}}\chi_{\text{e,He}}(z), \quad (3)$$

where $\chi_{\text{e,H}}(z)$ and $\chi_{\text{e,He}}(z)$ represent the ionization fractions of intergalactic hydrogen and helium, respectively, with mass fractions $Y_{\text{H}} = 3/4$ and $Y_{\text{p}} = 1/4$. For our calculations, we adopt $f_{\text{IGM}} = 0.85$ following [39]. The Hubble function $H(z)$ encodes the information of underlying cosmological model. Under the standard Λ

cold dark matter (Λ CDM) framework, neglecting contributions from radiation and curvature, it is given by $H(z) = H_0\sqrt{\Omega_m(1+z)^3 + \Omega_\Lambda}$, where Ω_m and Ω_Λ are the present-day matter and vacuum energy density fractions, respectively, constrained by the condition $\Omega_m + \Omega_\Lambda = 1$.

3. DATA SELECTION AND HUBBLE CONSTANT ESTIMATION

In this study, we analyze 64 FRBs that have been precisely localized within their host galaxies as of August 2024, which means their source redshifts (z_S) have been measured. The relevant observables of these FRBs are presented in Table 1. Considering the NE2001 model [40] of the Galactic distribution of free electrons, we present DM_{MW} for each of the bursts. As discussed in the previous section, DM_{Halo} is calculated based on the results of [37]. To account for the host galaxy's contribution to DM, we categorize these FRBs into two groups. For FRBs with reported DM_{Host} values, we directly use the maximum measured values. For those without available DM_{Host} data, we apply the model given in [38], as described earlier, to estimate the missing values. By substituting all these values into Equation (1), we calculate DM_{IGM} for each FRB.

TABLE 1: List of 64 localized FRBs as of August 2024 in chronological order. FRBs in bold indicate that their DM_{Host} values are reported. DM_{MW} is calculated based on NE2001 model.

Name	DM_{obs} (pc cm^{-3})	DM_{MW} (pc cm^{-3})	z_S	Repeater (Y/N)	Ref.
FRB 20121102A	557.0 ± 2.0	188.0	0.19273	Y	[7]
FRB 20171020A	114.1 ± 0.2	38.0	0.0086	N	[41]
FRB 20180301A	522.0 ± 0.2	152.0	0.3304	Y	[42]
FRB 20180916B	349.3 ± 0.2	200.0	0.0337	Y	[43]
FRB 20180924B	361.42 ± 0.06	40.5	0.3214	N	[44]
FRB 20181112A	589.27 ± 0.03	102.0	0.4755	N	[45]
FRB 20181220A	209.4 ± 0.1	126.0	0.02746	N	[46]
FRB 20181223C	112.5 ± 0.1	20.0	0.03024	N	[46]
FRB 20190102C	363.6 ± 0.3	57.3	0.291	N	[25]
FRB 20190110C	221.6 ± 1.6	37.1	0.12244	Y	[47]
FRB 20190303A	222.4 ± 0.7	29.0	0.064	Y	[48]
FRB 20190418A	184.5 ± 0.1	71.0	0.07132	N	[46]
FRB 20190425A	128.2 ± 0.1	49.0	0.03122	N	[46]
FRB 20190520B	1204.7 ± 10.0	113	0.241	Y	[49]
FRB 20190523A	760.8 ± 0.6	37.0	0.66	N	[50]
FRB 20190608B	338.7 ± 0.5	37.2	0.1178	N	[51]
FRB 20190611B	321.4 ± 0.2	57.83	0.3778	N	[52]
FRB 20190614D	959.2 ± 5.0	83.5	0.6	N	[53]
FRB 20190711A	593.1 ± 0.4	56.4	0.522	Y	[54]
FRB 20190714A	504.0 ± 2.0	39.0	0.2365	N	[52]
FRB 20191001A	506.92 ± 0.04	44.7	0.234	N	[55]
FRB 20191106C	332.2 ± 0.7	25.0	0.10775	Y	[47]
FRB 20191228A	297.50 ± 0.05	33.0	0.2432	N	[56]
FRB 20200223B	201.8 ± 0.4	45.6	0.0602	Y	[47]
FRB 20200430A	380.1 ± 0.4	27.0	0.16	N	[52]
FRB 20200906A	577.80 ± 0.02	36.0	0.3688	N	[56]
FRB 20201123A	433.55 ± 0.36	251.93	0.05	N	[57]

FRB 20201124A	413.52 ± 0.05	123.2	0.098	Y	[58]
FRB 20210117A	730.0 ± 1.0	34.4	0.2145	N	[59]
FRB 20210320C	384.8 ± 0.3	42.0	0.2797	N	[29]
FRB 20210405I	565.17 ± 0.49	516.1	0.066	N	[60]
FRB 20210410D	578.78 ± 2.00	56.2	0.1415	N	[61]
FRB 20210603A	500.147 ± 0.004	40.0	0.177	N	[62]
FRB 20210807D	251.9 ± 0.2	121.2	0.12927	N	[29]
FRB 20211127I	234.83 ± 0.08	42.5	0.0469	N	[29]
FRB 20211203C	636.2 ± 0.4	63.0	0.3437	N	[63]
FRB 20211212A	206.0 ± 5.0	27.1	0.0715	N	[29]
FRB 20220105A	583.0 ± 2.0	22.0	0.2785	N	[63]
FRB 20220207C	262.38 ± 0.01	79.3	0.04304	N	[64]
FRB 20220307B	499.27 ± 0.06	135.7	0.248123	N	[64]
FRB 20220310F	462.240 ± 0.005	45.4	0.477958	N	[64]
FRB 20220319D	110.95 ± 0.02	65.25	0.011	N	[65]
FRB 20220418A	623.25 ± 0.01	37.6	0.622	N	[64]
FRB 20220501C	449.5 ± 0.2	31.0	0.381	N	[63]
FRB 20220506D	396.97 ± 0.02	89.1	0.30039	N	[64]
FRB 20220509G	269.53 ± 0.02	55.2	0.0894	N	[64]
FRB 20220610A	1458.0 ± 0.2	31.0	1.017	N	[66]
FRB 20220725A	290.4 ± 0.3	31.0	0.1926	N	[63]
FRB 20220825A	651.24 ± 0.06	79.7	0.241397	N	[64]
FRB 20220912A	219.46 ± 0.04	125.0	0.077	Y	[67]
FRB 20220914A	631.28 ± 0.04	55.2	0.1139	N	[64]
FRB 20220918A	656.8 ± 0.4	41.0	0.491	N	[63]
FRB 20220920A	314.99 ± 0.01	40.3	0.158239	N	[64]
FRB 20221012A	441.08 ± 0.70	54.4	0.284669	N	[64]
FRB 20221106A	343.8 ± 0.8	35.0	0.2044	N	[63]
FRB 20230526A	361.4 ± 0.2	50.0	0.157	N	[63]
FRB 20230708A	411.51 ± 0.05	50.0	0.105	N	[63]
FRB 20230718A	476.6 ± 0.5	393.0	0.0357	N	[68]
FRB 20230902A	440.1 ± 0.1	34.0	0.3619	N	[63]
FRB 20231226A	329.9 ± 0.1	145.0	0.1569	N	[63]
FRB 20240114A	527.7 ± 0.1	40.0	0.42	Y	[69]
FRB 20240201A	374.5 ± 0.2	38.0	0.042729	N	[63]
FRB 20240210A	283.73 ± 0.05	31.0	0.023686	N	[63]
FRB 20240310A	601.8 ± 0.2	36.0	0.127	N	[63]

Figure 1 illustrates the z_S values of these FRBs plotted against their corresponding DM_{IGM} values, including error bars. The figure also shows the expected average $\langle DM_{\text{IGM}}(z_S) \rangle$ under the standard Λ CDM cosmology with $H_0 = 73 \text{ km s}^{-1} \text{ Mpc}^{-1}$, $\Omega_m = 0.30966$, $\Omega_\Lambda = 1 - \Omega_m$, and $\Omega_b = 0.04897$. Additionally, the 1σ and 2σ confidence regions for $\langle DM_{\text{IGM}}(z_S) \rangle$, derived from the results of [70] using the Illustris simulation, are depicted. These regions account for the inhomogeneous distribution of ionized gas in the IGM.

We now present our results on constraining H_0 using the analyzed data sample. The likelihood analysis is conducted within the Bayesian framework, utilizing the Markov chain Monte Carlo (MCMC) method in Python [71]. In particular, we select three distinct likelihood functions for this study to explore different modeling approaches.

3.1. Likelihood 1: incorporating uncertainties in DM_{IGM} measurements

We assume that the individual likelihood of DM_{IGM} for each FRB follows a Gaussian distribution, given by

$$P_i(DM_{\text{IGM},i} | z_{S,i}) = \frac{1}{\sqrt{2\pi\sigma_i^2}} e^{-\frac{(\langle DM_{\text{IGM}}(z_{S,i}) \rangle - DM_{\text{IGM},i})^2}{2\sigma_i^2}}. \quad (4)$$

where

$$\sigma_i^2 = \sigma_{\text{obs},i}^2 + \sigma_{\text{MW},i}^2 + \sigma_{\text{Halo},i}^2 + \sigma_{\text{IGM},i}^2 + \frac{\sigma_{\text{Host},i}^2}{1 + z_{S,i}}. \quad (5)$$

Here σ_{obs} is the error bar in the observed DM of each FRB, included in Table 1 and rests are error bars corresponding to each DM components. Thereby we define the joint likelihood function as

$$\mathcal{L} = \prod_{i=1}^{N_{\text{FRB}}} P_i(DM_{\text{IGM},i} | z_{S,i}), \quad (6)$$

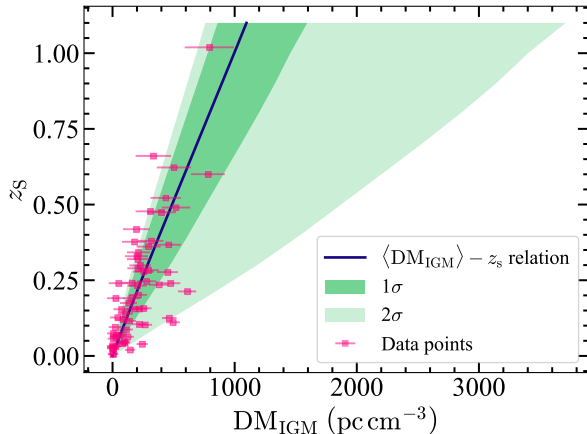


FIG. 1. The host redshift values for the localized FRBs are plotted against their estimated DM contribution from IGM along with their error bars. The black solid line depicts the $\langle \text{DM}_{\text{IGM}}(z_s) \rangle$ as a function of z_s assuming Λ CDM cosmology with $H_0 = 73 \text{ km s}^{-1} \text{ Mpc}^{-1}$, $\Omega_m = 0.30966$, $\Omega_\Lambda = 1 - \Omega_m$, and $\Omega_b = 0.04897$. Green shaded regions represent 1σ and 2σ confidence regions of DM_{IGM} .

where N_{FRB} is the total number of FRBs in the dataset. To obtain constraints on H_0 , the joint likelihood is maximized with respect to H_0 . As discussed previously, we adopt DM_{MW} values from NE2001 model, while its error bar is considered as $\sigma_{\text{MW}} = 30 \text{ pc cm}^{-3}$ [72]. For the Galactic halo, as it contributes $\text{DM}_{\text{Halo}} \approx 50 - 80 \text{ pc cm}^{-3}$, we draw values for each FRB from a uniform distribution $\mathcal{U}[50 - 80] \text{ pc cm}^{-3}$, and hence it indicates $\sigma_{\text{Halo}} = \sqrt{75} \text{ pc cm}^{-3}$. For host galaxy contributions, DM_{Host} is considered either from reported values or, if unavailable, from IllustrisTNG simulations, while we assume large scatter by considering $\sigma_{\text{Host}} = 50 \text{ pc cm}^{-3}$. The error bars in IGM component is considered from the simulated results in [70].

Figure 2 presents the probability density function of the joint likelihood for all 64 localized FRBs as a function of H_0 , along with the 1σ confidence region within the framework of Λ CDM cosmology. The likelihood is maximized at $H_0 = 70.42^{+3.73}_{-3.63} \text{ km s}^{-1} \text{ Mpc}^{-1}$, within the 1σ confidence level. This value represents the most robust constraint on H_0 derived from localized FRB data by comparing the calculated DM_{IGM} values with the mean $\langle \text{DM}_{\text{IGM}} \rangle$, based on the Macquart relation.

This estimate of H_0 is limited by the uncertainty in the host galaxy DM contributions. As previously mentioned, DM_{Host} of each FRB is either taken from its maximum reported value or from IllustrisTNG simulation, with the latter typically yielding lower values. It is currently impossible to accurately measure DM_{Host} for individual FRBs; however, its mean value, $\langle \text{DM}_{\text{Host}} \rangle$, can be estimated through MCMC analysis. By treating both H_0 and $\langle \text{DM}_{\text{Host}} \rangle$ as free parameters, we maximize the joint likelihood from Equation (6). Figure 3 shows the joint likelihood distribution, revealing a mean host DM con-

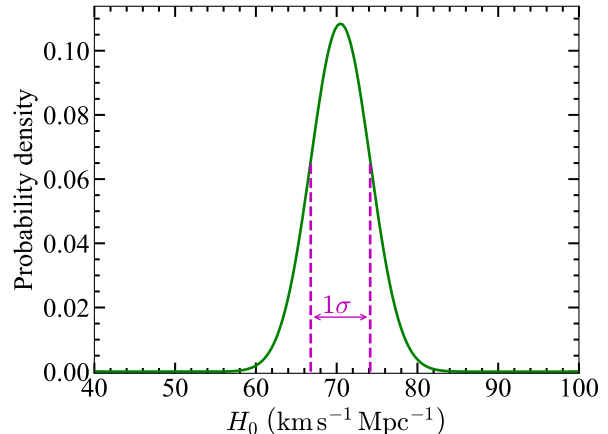


FIG. 2. Probability distribution of joint likelihood function of Equation (6) with respect to H_0 along with its 1σ confidence interval. The likelihood is maximized for $H_0 = 70.42^{+3.73}_{-3.63} \text{ km s}^{-1} \text{ Mpc}^{-1}$.

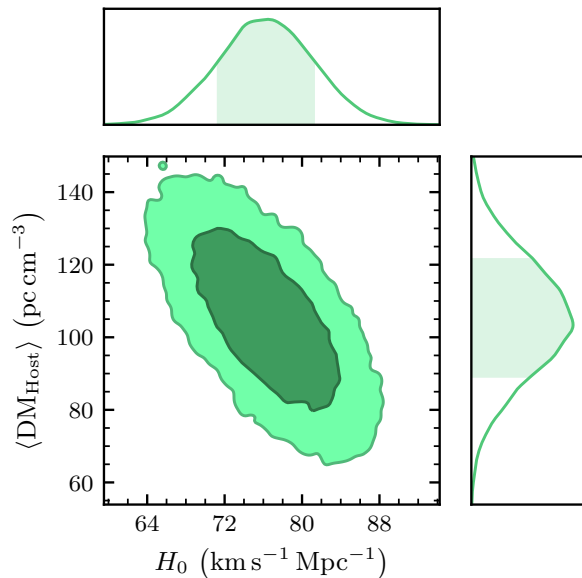


FIG. 3. 1σ and 2σ confidence regions of the joint likelihood of Equation (6) when it is optimized over both H_0 and $\langle \text{DM}_{\text{Host}} \rangle$. This likelihood is maximized for $H_0 = 76.26^{+4.86}_{-4.85} \text{ km s}^{-1} \text{ Mpc}^{-1}$ and $\langle \text{DM}_{\text{Host}} \rangle = 105.15^{+16.15}_{-15.77} \text{ pc cm}^{-3}$. This plot is prepared with ChainConsumer function of Python [73].

tribution of approximately $105.15^{+16.15}_{-15.77} \text{ pc cm}^{-3}$ and a revised Hubble constant of $H_0 = 76.26^{+4.86}_{-4.85} \text{ km s}^{-1} \text{ Mpc}^{-1}$. The error bars increase in this scenario, but it is noteworthy that this estimated H_0 aligns with values derived from late-time Universe supernovae data.

3.2. Likelihood 2: incorporating uncertainties in DM_{IGM} and DM_{Host} measurements

Given the substantial uncertainty in the host DM contribution, previously reported H_0 values should be interpreted with caution. To mitigate this uncertainty, we introduce a new likelihood function incorporating uncertainties in both DM_{IGM} and DM_{Host} . If $X(x)$, $Y(y)$, and $Z(z)$ are random variables ($x, y, z \geq 0$) with probability distributions $P_X(x)$, $P_Y(y)$, and $P_Z(z)$, respectively, such that $z = x + y$, then $P_Z(z) = \int_0^z P_X(x)P_Y(z-x) dx$. Applying this mathematical identity, we define the excess DM as $\text{DM}_{\text{exc}} = \text{DM} - \text{DM}_{\text{MW}} - \text{DM}_{\text{Halo}} = \text{DM}_{\text{IGM}} + \text{DM}_{\text{Host}}/(1 + z_S)$. We adopt the NE2001 model for DM_{MW} and a uniform distribution $\mathcal{U}[50 - 80] \text{ pc cm}^{-3}$ for DM_{Halo} to construct the following joint likelihood function [25]

$$\mathcal{L} = \prod_{i=1}^{N_{\text{FRB}}} P_i(\text{DM}_{\text{exc},i} | z_{S,i}), \quad (7)$$

which requires maximization over H_0 . Here

$$P_i(\text{DM}_{\text{exc},i} | z_{S,i}) = \int_0^{\text{DM}_{\text{exc},i}} P_{\text{Host}}\left(\frac{\text{DM}_{\text{Host}}}{1 + z_{S,i}}\right) \times P_{\text{IGM}}\left(\text{DM}_{\text{exc},i} - \frac{\text{DM}_{\text{Host}}}{1 + z_{S,i}}\right) d\text{DM}_{\text{Host}}. \quad (8)$$

Previous studies suggest that DM_{IGM} follows a specific probability distribution, given by [25]

$$P_{\text{IGM}}(\Delta_{\text{IGM}}) = A \Delta_{\text{IGM}}^{-\beta_2} e^{-\frac{(\Delta_{\text{IGM}}^{-\beta_1} - C_0)^2}{2\beta_1^2 \sigma_{\text{DM}}^2}}, \quad (9)$$

where $\Delta_{\text{IGM}} = \text{DM}_{\text{IGM}}/\langle \text{DM}_{\text{IGM}} \rangle$, σ_{DM} is its standard deviation, A , β_1 , β_2 , and C_0 are model parameters. We adopt the parameter values from [74], based on the IllustrisTNG simulation. The inherent difficulty in measuring DM_{Host} introduces significant uncertainty regarding its exact distribution. Following [25], we employ a log-normal probability distribution, given by

$$P_{\text{Host}}(\text{DM}_{\text{Host}}) = \frac{1}{\sqrt{2\pi} \text{DM}_{\text{Host}} \sigma_{\text{Host}}} e^{-\frac{(\ln \text{DM}_{\text{Host}} - \mu_{\text{Host}})^2}{2\sigma_{\text{Host}}^2}}, \quad (10)$$

with $e^{\mu_{\text{Host}}}$ being the median and $(e^{\sigma_{\text{Host}}^2} - 1) e^{2\mu_{\text{Host}} + \sigma_{\text{Host}}^2}$ its variance. Our analysis considers four different combinations of μ_{Host} and σ_{Host} , as listed in Table 2. These distribution functions effectively capture the uncertainties associated with DM_{IGM} and DM_{Host} values. Due to the precise localization of these FRBs, their redshift values are subject to minimal uncertainty.

Table 2 presents the values of H_0 with 1σ uncertainties for the four Host DM models. Figure 4 illustrates the

TABLE 2. Parameters involved in host DM probability distribution along with the estimated Hubble constant value in each case.

Model	$e^{\mu_{\text{Host}}}$	σ_{Host}	Ref.	H_0 (Likelihood 2) ($\text{km s}^{-1} \text{Mpc}^{-1}$)	H_0 (Likelihood 3) ($\text{km s}^{-1} \text{Mpc}^{-1}$)
Model I	66	0.42	[25]	$74.77^{+2.51}_{-2.65}$	$77.23^{+2.62}_{-2.71}$
Model II	30	0.17	[75]	$73.41^{+2.28}_{-2.71}$	$76.52^{+2.65}_{-2.57}$
Model III	130	0.53	[29]	$73.74^{+2.43}_{-2.77}$	$76.16^{+2.48}_{-2.89}$
Model IV	$f(z_S)^*$	$f(z_S)^*$	[38]	$83.53^{+2.32}_{-2.92}$	$85.08^{+2.71}_{-2.66}$

*In model IV, $e^{\mu_{\text{Host}}}$ and σ_{Host} change with the host redshift; hence we do not mention any values in the table.

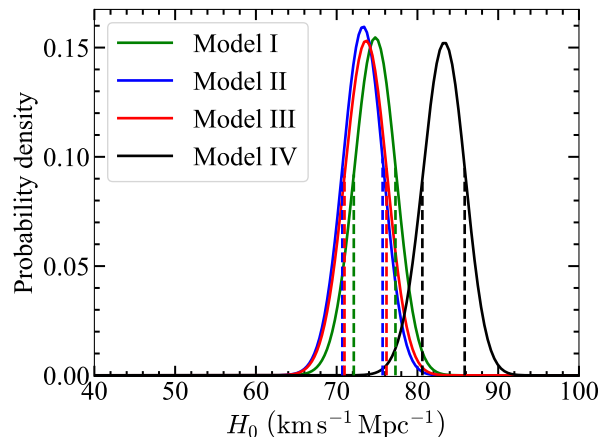


FIG. 4. Probability distribution of joint likelihood function of Equation (7) with respect to H_0 along with its 1σ confidence interval for four different host DM models.

probability distribution of the joint likelihood function of Equation (6) with respect to H_0 , along with its 1σ confidence interval for each host DM model. Except for Model IV, the other three models yield similar H_0 . Notably, the error bars decrease to approximately $\pm 2.5 \text{ km s}^{-1} \text{Mpc}^{-1}$ compared to those obtained using likelihood 1 in the aforementioned section. All these H_0 values are consistent with the SH0ES collaboration result for nearby SNe Ia [36] and the reduced 1σ uncertainty error bars no longer overlap with H_0 value derived from CMB data.

It is important to note that FRB data alone cannot definitively predict the value of H_0 . This limitation primarily stems from the significant uncertainties in DM_{IGM} and DM_{Host} . As depicted in Figure 4, different host DM models, characterized by varying combinations of $e^{\mu_{\text{Host}}}$ and σ_{Host} , produce distinct results. Therefore, host DM modeling plays a crucial role in determining the H_0 value. By exploring numerous combinations of these two model parameters, we plot the corresponding H_0 values in Figure 5. The results demonstrate that various combinations of $e^{\mu_{\text{Host}}}$ and σ_{Host} can yield same H_0 . Furthermore, we observe that a scenario with a high host DM component and low scatter in their DM values, represented by high $e^{\mu_{\text{Host}}}$ and low σ_{Host} , leads to very low H_0 estimates. Such a scenario is highly unrealistic, as FRBs originate from diverse environments, including

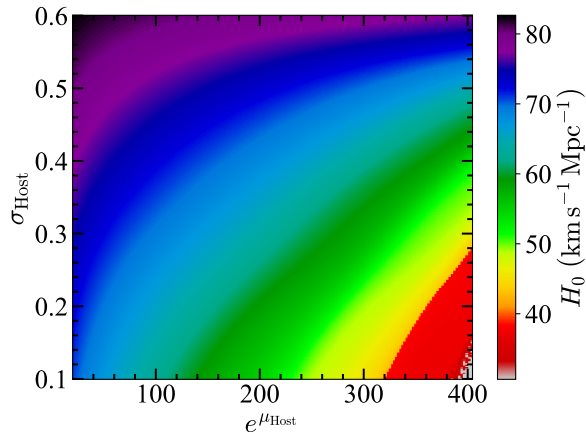


FIG. 5. Values of Hubble constant, indicated by the color bar, estimated using likelihood of Equation (7) for different combinations of $e^{\mu_{\text{Host}}}$ and σ_{Host} in host DM model.

galaxies with varying morphologies, star formation rates, and other properties. Thus, in general, we can expect to have large σ_{Host} in their distribution. Conversely, if σ_{Host} is reasonably high, H_0 is estimated to be around or above $70 \text{ km s}^{-1} \text{ Mpc}^{-1}$, which is consistent with values obtained from different realistic simulations as listed in Table 2.

3.3. Likelihood 3: incorporating uncertainties in DM_{IGM} , DM_{Host} , and DM_{Halo} measurements

While the Milky Way’s DM can be reasonably modeled using either NE2001 [40] or YMW16 [76] models, the values of the halo DM contribution remain uncertain. Although previous studies have suggested $\text{DM}_{\text{Halo}} \approx 50 - 80 \text{ pc cm}^{-3}$ [37], the exact value for each FRB is unknown. Unlike the uncertainty in host DM contributions, the scatter in DM_{Halo} is relatively small, and we anticipate minor improvements in results due to this variation. We now investigate the impact of the DM_{Halo} uncertainty on the H_0 estimation.

Defining $\text{DM}' = \text{DM} - \text{DM}_{\text{MW}} = \text{DM}_{\text{exc}} + \text{DM}_{\text{Halo}}$, we take into account this uncertainty in the modified likelihood function, given by

$$\mathcal{L} = \prod_{i=1}^{N_{\text{FRB}}} P_i(\text{DM}'_i | z_{S,i}), \quad (11)$$

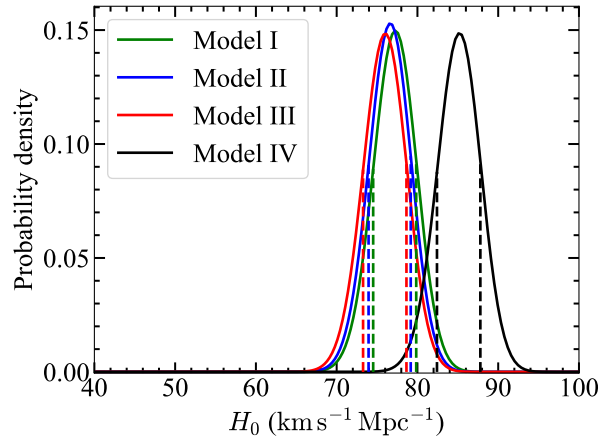


FIG. 6. Probability distribution of joint likelihood function of Equation (11) with respect to H_0 together with its 1σ confidence interval for four different host DM models.

where

$$P_i(\text{DM}'_i | z_{S,i}) = \int_0^{\text{DM}'_i} \int_0^{\text{DM}'_i - \text{DM}_{\text{Halo}}} P_{\text{Halo}}(\text{DM}_{\text{Halo}}) \times P_{\text{IGM}}\left(\text{DM}'_i - \frac{\text{DM}_{\text{Host}}}{1 + z_{S,i}} - \text{DM}_{\text{Halo}}\right) \times P_{\text{Host}}\left(\frac{\text{DM}_{\text{Host}}}{1 + z_{S,i}}\right) d\text{DM}_{\text{Halo}} d\text{DM}_{\text{Host}}. \quad (12)$$

We model the probability distribution of DM_{Halo} , $P_{\text{Halo}}(\text{DM}_{\text{Halo}})$, as a Gaussian distribution with mean μ_{Halo} and standard deviation σ_{Halo} , as follows:

$$P_{\text{Halo}}(\text{DM}_{\text{Halo}}) = \frac{1}{\sqrt{2\pi\sigma_{\text{Halo}}^2}} e^{-\frac{(\text{DM}_{\text{Halo}} - \mu_{\text{Halo}})^2}{2\sigma_{\text{Halo}}^2}}. \quad (13)$$

Assuming $\mu_{\text{Halo}} \approx 65 \text{ pc cm}^{-3}$ and $\sigma_{\text{Halo}} \approx 5 \text{ pc cm}^{-3}$, we can mimic the cumulative function of this Gaussian distribution with the previously assumed uniform distribution $\mathcal{U}[50 - 80] \text{ pc cm}^{-3}$. Figure 6 illustrates the probability densities as a function of H_0 , along with 1σ confidence intervals for all four host DM models discussed in the previous section. The H_0 values at which the distributions are maximized are listed in the last column of Table 2. As expected, the values exhibit slight deviations with the introduction of DM_{Halo} uncertainty, although there is no significant improvement in error bars.

4. DISCUSSION

One of the most pressing challenges in modern cosmology is the Hubble tension, which refers to the discrepancy between two independent sets of measurements of the Universe’s current expansion rate, yielding different values for H_0 . The first method relies on observations

of the CMB as measured by missions like Planck. These early-Universe observations, combined with the Λ CDM model, predict a value of $H_0 = 67.36 \pm 0.54 \text{ km s}^{-1} \text{ Mpc}^{-1}$ [77]. The second method involves directly measuring the expansion rate in the local Universe by observing the redshifts of SNe Ia and other distance indicators like Cepheid variable stars. These late-Universe measurements consistently yield a higher value of $H_0 = 73.04 \pm 1.04 \text{ km s}^{-1} \text{ Mpc}^{-1}$ [36]. This statistically significant mismatch, known as the Hubble tension, suggests potential gaps in our understanding of cosmology. Several proposed solutions to this tension include exploring dynamical dark energy models, utilizing new cosmic probes like GWs, improving the calibration of distance indicators using gravitational lensing, and other approaches (see comprehensive discussions in [78] and [79]). Ultimately, resolving the Hubble tension will likely require a combination of more precise observations and potentially a revision of the current cosmological framework.

To address this challenge, we consider FRBs as a potential tool for estimating H_0 . There are relatively recent studies conducted previously in this direction as mentioned in the Introduction. However, due to their consideration of fewer FRBs, they all have large error bars in their estimations of H_0 . These error bars can, in principle, take into account for both H_0 obtained for the early- and late-time Universe cosmology, ultimately preventing to draw any decisive conclusion on the Hubble tension. In our study, we consider a larger sample of 64 extragalactic, localized FRBs from various telescopes. Employing Bayesian analysis with three different likelihood functions, we consistently obtain H_0 values well above $70 \text{ km s}^{-1} \text{ Mpc}^{-1}$, aligning with the late-Universe H_0 values. This is expected as the FRBs are localized to a maximum redshift of around 1, consistent with the typical redshifts considered in late-time Universe studies. It is noteworthy our estimated H_0 values have significantly reduced error bars of approximately $\pm 2.5 \text{ km s}^{-1} \text{ Mpc}^{-1}$, clearly distinguishing them from the early-Universe H_0 , unlike previous FRB studies. Although the error bars may not be as tight as those derived from SNe Ia data, they are considerably smaller than those obtained from GW astronomy, demonstrating the potential of FRBs as a promising cosmological probe.

An important point to highlight is that the value of H_0 derived from FRB data is dependent on the underlying cosmological model. In our study, we have employed the Λ CDM framework. However, in the literature, various cosmological models have been considered, particularly in efforts to address the Hubble tension. One simple model involves a dynamical dark energy equation of state, defined as $w \equiv P/\rho$ where P and ρ represent pressure and energy density, respectively. A dynamical dark energy model has the potential to alleviate both the Hubble tension and the σ_8 tension simultaneously [78, 80, 81]. To exemplify, we assume that the dark energy equation of state evolves over time, such that the time-dependent Hubble parameter

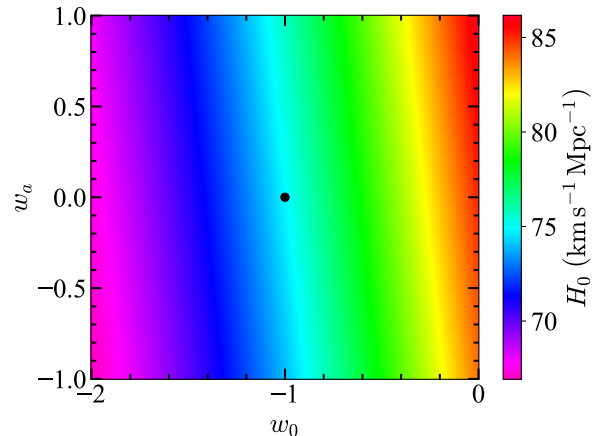


FIG. 7. Variation of H_0 for different dark energy equation of states considering Model I for host galaxy DM distribution. The colorbar shows H_0 for different combinations of w_0 and w_a . The black point at the center corresponds to the Hubble constant value in Λ CDM cosmology.

can be expressed as $H(z) = H_0 \sqrt{\Omega_m (1+z)^3 + \Omega_\Lambda f(z)}$ [82], where $f(z) = (1+z)^{3(1+w_0+w_a)} \exp\{-3w_a z/(1+z)\}$ with w_0 and w_a being dimensionless parameters, and $w(z) = w_0 + w_a z/(1+z)$. It is clear that for $w_0 = -1$ and $w_a = 0$ the standard Λ CDM cosmology with $w = -1$ is recovered. However, other parameter combinations can lead to $w(z) < -1$ for certain redshifts which is usually excluded as a theory cut is made at $w(z) = -1$. This alteration to the cosmological model also influences $\langle \text{DM}_{\text{IGM}}(z) \rangle$, which subsequently affects the likelihood functions. Figure 7 shows the estimated H_0 using the joint likelihood function of Equation (7), assuming Model I for host DM distribution and different combinations of w_0 and w_a . We observe that, for certain parameter combinations, H_0 can be closer to the values predicted by early-Universe cosmology.

5. CONCLUSIONS

In this study, we have explored the potential of FRBs as a tool for constraining the Hubble constant. Despite uncertainties in DM_{IGM} and DM_{Host} quantities, we have demonstrated that FRBs can serve as a valuable cosmological probe. By analyzing a dataset of 64 extragalactic, localized FRBs, we have consistently derived H_0 values exceeding $70 \text{ km s}^{-1} \text{ Mpc}^{-1}$, in agreement with the late-Universe Hubble constant estimates. Our results exhibit significantly reduced error bars, approximately $\pm 2.5 \text{ km s}^{-1} \text{ Mpc}^{-1}$, further distinguishing them from early-Universe measurements. These findings emphasize the potential of FRBs to contribute to cosmological parameter constraints and highlight the ongoing Hubble tension.

Numerous cosmological probes and methods are cur-

rently under investigation to resolve the tensions in cosmology and enhance the precision of cosmological measurements. Gamma-Ray Bursts, Quasars, and Active Galactic Nuclei are being explored as potential standardizable candles to enable more accurate distance measurements. Alternatively, BAOs are also being explored to use as standard ruler. Furthermore, novel approaches such as machine learning techniques and model-independent methods are being utilized to analyze large datasets and mitigate systematic biases. Independent methodologies, including Cosmic Chronometers and GW standard sirens, are also providing alternative measurements of the Universe's expansion rate. These advances aim to improve our understanding of key cosmological parameters and help resolve the H_0 discrepancy.

Upcoming surveys, such as Canadian Hydrogen Observatory and Radio-transient Detector (CHORD)⁴, Hydrogen Intensity and Real-time Analysis eXperiment (HIRAX)⁵, Square Kilometre Array (SKA)⁶, Deep Synoptic Array (DSA)-2000⁷, and Bustling Universe Radio Survey Telescope in Taiwan (BURSTT)⁸ are expected to detect a larger number of FRBs, with a significant fraction localized to their host galaxies. These surveys promise to deliver more stringent constraints on cosmological parameters, potentially offering critical insights into the Hubble

tension. In conclusion, our study underscores the potential of FRBs as a powerful tool for probing the large-scale structure of the Universe. As research in this field continues to advance, we anticipate that FRBs will play an increasingly prominent role in refining our understanding of the cosmos, from the properties of IGM to the determination of fundamental cosmological parameters.

ACKNOWLEDGMENTS

S.K. would like to thank S. Hagstotz of Ludwig Maximilian University of Munich for valuable discussions and providing their code for generating mock catalog of FRBs. We gratefully acknowledge support from the University of Cape Town Vice Chancellor's Future Leaders 2030 Awards programme which has generously funded this research and support from the South African Research Chairs Initiative of the Department of Science and Technology and the National Research Foundation. A.W. would like to acknowledge support from the ICTP through the Associates Programme and from the Simons Foundation through grant number 284558FY19. Computations were performed using facilities provided by the University of Cape Town's ICTS High Performance Computing team: hpc.uct.ac.za [83].

-
- [1] D.R. Lorimer, M. Bailes, M.A. McLaughlin, D.J. Narkevic and F. Crawford, *A Bright Millisecond Radio Burst of Extragalactic Origin*, *Science* **318** (2007) 777 [0709.4301].
- [2] Z. Pleunis, D. Michilli, C.G. Bassa, J.W.T. Hessels, A. Naidu, B.C. Andersen et al., *LOFAR Detection of 110-188 MHz Emission and Frequency-dependent Activity from FRB 20180916B*, *Astrophys. J. Lett.* **911** (2021) L3 [2012.08372].
- [3] V. Gajjar, A.P.V. Siemion, D.C. Price, C.J. Law, D. Michilli, J.W.T. Hessels et al., *Highest Frequency Detection of FRB 121102 at 4-8 GHz Using the Breakthrough Listen Digital Backend at the Green Bank Telescope*, *Astrophys. J.* **863** (2018) 2 [1804.04101].
- [4] C.D. Bochenek, D.L. McKenna, K.V. Belov, J. Kocz, S.R. Kulkarni, J. Lamb et al., *STARE2: Detecting Fast Radio Bursts in the Milky Way*, *Publ. Astron. Soc. Pac.* **132** (2020) 034202 [2001.05077].
- [5] C.D. Bochenek, V. Ravi, K.V. Belov, G. Hallinan, J. Kocz, S.R. Kulkarni et al., *A fast radio burst associated with a Galactic magnetar*, *Nature* **587** (2020) 59 [2005.10828].
- [6] CHIME/FRB Collaboration, B.C. Andersen, K.M. Bandura, M. Bhardwaj, A. Bij, M.M. Boyce et al., *A bright millisecond-duration radio burst from a Galactic magnetar*, *Nature* **587** (2020) 54 [2005.10324].
- [7] S.P. Tendulkar, C.G. Bassa, J.M. Cordes, G.C. Bower, C.J. Law, S. Chatterjee et al., *The Host Galaxy and Redshift of the Repeating Fast Radio Burst FRB 121102*, *Astrophys. J. Lett.* **834** (2017) L7 [1701.01100].
- [8] Y. Lyubarsky, *A model for fast extragalactic radio bursts*, *Mon. Not. Roy. Astron. Soc.* **442** (2014) L9 [1401.6674].
- [9] E. Platts, A. Weltman, A. Walters, S.P. Tendulkar, J.E.B. Gordin and S. Kandhai, *A living theory catalogue for fast radio bursts*, *Phys. Rep.* **821** (2019) 1 [1810.05836].
- [10] B. Zhang, *The physical mechanisms of fast radio bursts*, *Nature* **587** (2020) 45 [2011.03500].
- [11] S. Kalita and A. Weltman, *Continuous gravitational wave detection to understand the generation mechanism of fast radio bursts*, *Mon. Not. Roy. Astron. Soc.* **520** (2023) 3742 [2211.00940].
- [12] L. Bonetti, J. Ellis, N.E. Mavromatos, A.S. Sakharov, E.K. Sarkisyan-Grinbaum and A.D.A.M. Spallicci, *Photon mass limits from fast radio bursts*, *Physics Letters B* **757** (2016) 548 [1602.09135].
- [13] H. Wang, X. Miao and L. Shao, *Bounding the photon mass with cosmological propagation of fast radio bursts*, *Physics Letters B* **820** (2021) 136596 [2103.15299].
- [14] H.-N. Lin, L. Tang and R. Zou, *Revised constraints on the photon mass from well-localized fast radio bursts*, *Mon. Not. Roy. Astron. Soc.* **520** (2023) 1324 [2301.12103].

⁴ <https://www.chord-observatory.ca/>

⁵ <https://hirax.ukzn.ac.za/>

⁶ <https://www.skao.int/en>

⁷ <https://www.deepsynoptic.org/overview>

⁸ <https://www.burstt.org/>

- [15] J.B. Muñoz, E.D. Kovetz, L. Dai and M. Kamionkowski, *Lensing of Fast Radio Bursts as a Probe of Compact Dark Matter*, *Phys. Rev. Lett.* **117** (2016) 091301 [1605.00008].
- [16] M.W. Sammons, J.-P. Macquart, R.D. Ekers, R.M. Shannon, H. Cho, J.X. Prochaska et al., *First Constraints on Compact Dark Matter from Fast Radio Burst Microstructure*, *Astrophys. J.* **900** (2020) 122 [2002.12533].
- [17] R. Laha, *Lensing of fast radio bursts: Future constraints on primordial black hole density with an extended mass function and a new probe of exotic compact fermion and boson stars*, *Phys. Rev. D* **102** (2020) 023016 [1812.11810].
- [18] K. Liao, S.B. Zhang, Z. Li and H. Gao, *Constraints on Compact Dark Matter with Fast Radio Burst Observations*, *Astrophys. J. Lett.* **896** (2020) L11 [2003.13349].
- [19] C. Leung, Z. Kader, K.W. Masui, M. Dobbs, D. Michilli, J. Mena-Parra et al., *Constraining primordial black holes using fast radio burst gravitational-lens interferometry with CHIME/FRB*, *Phys. Rev. D* **106** (2022) 043017 [2204.06001].
- [20] S. Kalita, S. Bhatporia and A. Weltman, *Gravitational lensing in modified gravity: a case study for Fast Radio Bursts*, *J. Cosmol. Astropart. Phys.* **2023** (2023) 059 [2308.16604].
- [21] R. Reischke and S. Hagstotz, *Consistent constraints on the equivalence principle from localized fast radio bursts*, *Mon. Not. Roy. Astron. Soc.* **523** (2023) 6264 [2302.10072].
- [22] S. Kalita, *Constraining fundamental constants with fast radio bursts: unveiling the role of energy scale*, *Mon. Not. Roy. Astron. Soc.* **533** (2024) L57 [2407.01736].
- [23] T. Lemos, R. Gonçalves, J. Carvalho and J. Alcaniz, *A search for the fine-structure constant evolution from fast radio bursts and type Ia supernovae data*, *arXiv e-prints* (2024) arXiv:2406.11691 [2406.11691].
- [24] A. Walters, A. Weltman, B.M. Gaensler, Y.-Z. Ma and A. Witzemann, *Future Cosmological Constraints From Fast Radio Bursts*, *Astrophys. J.* **856** (2018) 65 [1711.11277].
- [25] J.P. Macquart, J.X. Prochaska, M. McQuinn, K.W. Bannister, S. Bhandari, C.K. Day et al., *A census of baryons in the Universe from localized fast radio bursts*, *Nature* **581** (2020) 391 [2005.13161].
- [26] Z.-X. Li, H. Gao, X.-H. Ding, G.-J. Wang and B. Zhang, *Strongly lensed repeating fast radio bursts as precision probes of the universe*, *Nature Communications* **9** (2018) 3833 [1708.06357].
- [27] S. Hagstotz, R. Reischke and R. Lilow, *A new measurement of the Hubble constant using fast radio bursts*, *Mon. Not. Roy. Astron. Soc.* **511** (2022) 662 [2104.04538].
- [28] Q. Wu, G.-Q. Zhang and F.-Y. Wang, *An 8 per cent determination of the Hubble constant from localized fast radio bursts*, *Mon. Not. Roy. Astron. Soc.* **515** (2022) L1 [2108.00581].
- [29] C.W. James, E.M. Ghosh, J.X. Prochaska, K.W. Bannister, S. Bhandari, C.K. Day et al., *A measurement of Hubble's Constant using Fast Radio Bursts*, *Mon. Not. Roy. Astron. Soc.* **516** (2022) 4862 [2208.00819].
- [30] J. Baptista, J.X. Prochaska, A.G. Mannings, C.W. James, R.M. Shannon, S.D. Ryder et al., *Measuring the Variance of the Macquart Relation in Redshift-Extragalactic Dispersion Measure Modeling*, *Astrophys. J.* **965** (2024) 57 [2305.07022].
- [31] Y. Liu, H. Yu and P. Wu, *Cosmological-model-independent Determination of Hubble Constant from Fast Radio Bursts and Hubble Parameter Measurements*, *Astrophys. J. Lett.* **946** (2023) L49 [2210.05202].
- [32] J.-J. Wei and F. Melia, *Investigating Cosmological Models and the Hubble Tension Using Localized Fast Radio Bursts*, *Astrophys. J.* **955** (2023) 101 [2308.05918].
- [33] Z.-W. Zhao, J.-G. Zhang, Y. Li, J.-F. Zhang and X. Zhang, *FRB dark sirens: Measuring the Hubble constant with unlocalized fast radio bursts*, *arXiv e-prints* (2022) arXiv:2212.13433 [2212.13433].
- [34] J. Gao, Z. Zhou, M. Du, R. Zou, J. Hu and L. Xu, *A measurement of Hubble constant using cosmographic approach combining fast radio bursts and supernovae*, *Mon. Not. Roy. Astron. Soc.* **527** (2024) 7861 [2307.08285].
- [35] J.A.S. Fortunato, D.J. Bacon, W.S. Hipólito-Ricaldi and D. Wands, *Fast Radio Bursts and Artificial Neural Networks: a cosmological-model-independent estimation of the Hubble Constant*, *arXiv e-prints* (2024) arXiv:2407.03532 [2407.03532].
- [36] A.G. Riess, W. Yuan, L.M. Macri, D. Scolnic, D. Brout, S. Casertano et al., *A Comprehensive Measurement of the Local Value of the Hubble Constant with 1 km s^{-1} Mpc $^{-1}$ Uncertainty from the Hubble Space Telescope and the SH0ES Team*, *Astrophys. J. Lett.* **934** (2022) L7 [2112.04510].
- [37] J.X. Prochaska and Y. Zheng, *Probing Galactic haloes with fast radio bursts*, *Mon. Not. Roy. Astron. Soc.* **485** (2019) 648 [1901.11051].
- [38] G.Q. Zhang, H. Yu, J.H. He and F.Y. Wang, *Dispersion Measures of Fast Radio Burst Host Galaxies Derived from IllustrisTNG Simulation*, *Astrophys. J.* **900** (2020) 170 [2007.13935].
- [39] J.M. Cordes, S.K. Ocker and S. Chatterjee, *Redshift Estimation and Constraints on Intergalactic and Interstellar Media from Dispersion and Scattering of Fast Radio Bursts*, *Astrophys. J.* **931** (2022) 88 [2108.01172].
- [40] J.M. Cordes and T.J.W. Lazio, *NE2001.I. A New Model for the Galactic Distribution of Free Electrons and its Fluctuations*, *arXiv e-prints* (2002) astro [astro-ph/0207156].
- [41] E.K. Mahony, R.D. Ekers, J.-P. Macquart, E.M. Sadler, K.W. Bannister, S. Bhandari et al., *A Search for the Host Galaxy of FRB 171020*, *Astrophys. J. Lett.* **867** (2018) L10 [1810.04354].
- [42] D.C. Price, G. Foster, M. Geyer, W. van Straten, V. Gajjar, G. Hellbourg et al., *A fast radio burst with frequency-dependent polarization detected during Breakthrough Listen observations*, *Mon. Not. Roy. Astron. Soc.* **486** (2019) 3636 [1901.07412].
- [43] B. Marcote, K. Nimmo, J.W.T. Hessels, S.P. Tendulkar, C.G. Bassa, Z. Paragi et al., *A repeating fast radio burst source localized to a nearby spiral galaxy*, *Nature* **577** (2020) 190 [2001.02222].

- [44] K.W. Bannister, A.T. Deller, C. Phillips, J.P. Macquart, J.X. Prochaska, N. Tejos et al., *A single fast radio burst localized to a massive galaxy at cosmological distance*, *Science* **365** (2019) 565 [1906.11476].
- [45] J.X. Prochaska, J.-P. Macquart, M. McQuinn, S. Simha, R.M. Shannon, C.K. Day et al., *The low density and magnetization of a massive galaxy halo exposed by a fast radio burst*, *Science* **366** (2019) 231 [1909.11681].
- [46] M. Bhardwaj, D. Michilli, A.Y. Kirichenko, O. Modilim, K. Shin, V.M. Kaspi et al., *Host Galaxies for Four Nearby CHIME/FRB Sources and the Local Universe FRB Host Galaxy Population*, *Astrophys. J. Lett.* **971** (2024) L51 [2310.10018].
- [47] A.L. Ibig, M.R. Drout, B.M. Gaensler, P. Scholz, D. Michilli, M. Bhardwaj et al., *Proposed Host Galaxies of Repeating Fast Radio Burst Sources Detected by CHIME/FRB*, *Astrophys. J.* **961** (2024) 99 [2304.02638].
- [48] D. Michilli, M. Bhardwaj, C. Brar, B.M. Gaensler, V.M. Kaspi, A. Kirichenko et al., *Subarcminute Localization of 13 Repeating Fast Radio Bursts Detected by CHIME/FRB*, *Astrophys. J.* **950** (2023) 134 [2212.11941].
- [49] S.K. Ocker, J.M. Cordes, S. Chatterjee, C.-H. Niu, D. Li, J.W. McKee et al., *The Large Dispersion and Scattering of FRB 20190520B Are Dominated by the Host Galaxy*, *Astrophys. J.* **931** (2022) 87 [2202.13458].
- [50] N. Pol, M.T. Lam, M.A. McLaughlin, T.J.W. Lazio and J.M. Cordes, *Estimates of Fast Radio Burst Dispersion Measures from Cosmological Simulations*, *Astrophys. J.* **886** (2019) 135 [1903.07630].
- [51] S. Simha, J.N. Burchett, J.X. Prochaska, J.S. Chittidi, O. Elek, N. Tejos et al., *Disentangling the Cosmic Web toward FRB 190608*, *Astrophys. J.* **901** (2020) 134 [2005.13157].
- [52] K.E. Heintz, J.X. Prochaska, S. Simha, E. Platts, W.-f. Fong, N. Tejos et al., *Host Galaxy Properties and Offset Distributions of Fast Radio Bursts: Implications for Their Progenitors*, *Astrophys. J.* **903** (2020) 152 [2009.10747].
- [53] C.J. Law, B.J. Butler, J.X. Prochaska, B. Zackay, S. Burke-Spolaor, A. Mannings et al., *A Distant Fast Radio Burst Associated with Its Host Galaxy by the Very Large Array*, *Astrophys. J.* **899** (2020) 161 [2007.02155].
- [54] P. Kumar, R.M. Shannon, C. Flynn, S. Osłowski, S. Bhandari, C.K. Day et al., *Extremely band-limited repetition from a fast radio burst source*, *Mon. Not. Roy. Astron. Soc.* **500** (2021) 2525 [2009.01214].
- [55] E. Kundu, *Is FRB 191001 embedded in a supernova remnant?*, *Mon. Not. Roy. Astron. Soc.* **512** (2022) L1 [2201.03723].
- [56] S. Bhandari, K.E. Heintz, K. Aggarwal, L. Marnoch, C.K. Day, J. Sydnor et al., *Characterizing the Fast Radio Burst Host Galaxy Population and its Connection to Transients in the Local and Extragalactic Universe*, *Astron. J.* **163** (2022) 69 [2108.01282].
- [57] K.M. Rajwade, M.C. Bezuidenhout, M. Caleb, L.N. Driessen, F. Jankowski, M. Malenta et al., *First discoveries and localizations of Fast Radio Bursts with MeerTRAP: real-time, commensal MeerKAT survey*, *Mon. Not. Roy. Astron. Soc.* **514** (2022) 1961 [2205.14600].
- [58] V. Ravi, C.J. Law, D. Li, K. Aggarwal, M. Bhardwaj, S. Burke-Spolaor et al., *The host galaxy and persistent radio counterpart of FRB 20201124A*, *Mon. Not. Roy. Astron. Soc.* **513** (2022) 982 [2106.09710].
- [59] S. Bhandari, A.C. Gordon, D.R. Scott, L. Marnoch, N. Sridhar, P. Kumar et al., *A Nonrepeating Fast Radio Burst in a Dwarf Host Galaxy*, *Astrophys. J.* **948** (2023) 67 [2211.16790].
- [60] L.N. Driessen, E.D. Barr, D.A.H. Buckley, M. Caleb, H. Chen, W. Chen et al., *FRB 20210405I: a nearby Fast Radio Burst localized to sub-arcsecond precision with MeerKAT*, *Mon. Not. Roy. Astron. Soc.* **527** (2024) 3659 [2302.09787].
- [61] M. Caleb, L.N. Driessen, A.C. Gordon, N. Tejos, L. Bernales, H. Qiu et al., *A subarcsec localized fast radio burst with a significant host galaxy dispersion measure contribution*, *Mon. Not. Roy. Astron. Soc.* **524** (2023) 2064 [2302.09754].
- [62] T. Cassanelli, C. Leung, P. Sanghavi, J. Mena-Parra, S. Cary, R. Mckinven et al., *A fast radio burst localized at detection to a galactic disk using very long baseline interferometry*, *arXiv e-prints* (2023) arXiv:2307.09502 [2307.09502].
- [63] R.M. Shannon, K.W. Bannister, A. Bera, S. Bhandari, C.K. Day, A.T. Deller et al., *The Commensal Real-time ASKAP Fast Transient incoherent-sum survey*, *arXiv e-prints* (2024) arXiv:2408.02083 [2408.02083].
- [64] C.J. Law, K. Sharma, V. Ravi, G. Chen, M. Catha, L. Connor et al., *Deep Synoptic Array Science: First FRB and Host Galaxy Catalog*, *Astrophys. J.* **967** (2024) 29 [2307.03344].
- [65] V. Ravi, M. Catha, G. Chen, L. Connor, J.M. Cordes, J.T. Faber et al., *Deep Synoptic Array science: a 50 Mpc fast radio burst constrains the mass of the Milky Way circumgalactic medium*, *arXiv e-prints* (2023) arXiv:2301.01000 [2301.01000].
- [66] A.C. Gordon, W.-f. Fong, S. Simha, Y. Dong, C.D. Kilpatrick, A.T. Deller et al., *A Fast Radio Burst in a Compact Galaxy Group at $z \sim 1$* , *Astrophys. J. Lett.* **963** (2024) L34 [2311.10815].
- [67] V. Ravi, M. Catha, G. Chen, L. Connor, J.T. Faber, J.W. Lamb et al., *Deep Synoptic Array Science: Discovery of the Host Galaxy of FRB 20220912A*, *Astrophys. J. Lett.* **949** (2023) L3 [2211.09049].
- [68] M. Glowacki, A. Bera, K. Lee-Waddell, A.T. Deller, T. Dial, K. Gourdji et al., *H I, FRB, What's Your z: The First FRB Host Galaxy Redshift from Radio Observations*, *Astrophys. J. Lett.* **962** (2024) L13 [2311.16808].
- [69] A. Kumar, Y. Maan and Y. Bhusare, *Varying activity and the bursts properties of FRB 20240114A probed with GMRT down to 300 MHz*, *arXiv e-prints* (2024) arXiv:2406.12804 [2406.12804].
- [70] M. Jaroszynski, *Fast radio bursts and cosmological tests*, *Mon. Not. Roy. Astron. Soc.* **484** (2019) 1637 [1812.11936].
- [71] D. Foreman-Mackey, D.W. Hogg, D. Lang and J. Goodman, *emcee: The MCMC Hammer*, *Publ. Astron. Soc. Pac.* **125** (2013) 306 [1202.3665].
- [72] R.N. Manchester, G.B. Hobbs, A. Teoh and M. Hobbs, *The Australia Telescope National Facility Pulsar Catalogue*, *Astron. J.* **129** (2005) 1993 [astro-ph/0412641].

- [73] S.R. Hinton, *ChainConsumer*, *The Journal of Open Source Software* **1** (2016) 00045.
- [74] Z.J. Zhang, K. Yan, C.M. Li, G.Q. Zhang and F.Y. Wang, *Intergalactic Medium Dispersion Measures of Fast Radio Bursts Estimated from IllustrisTNG Simulation and Their Cosmological Applications*, *Astrophys. J.* **906** (2021) 49 [2011.14494].
- [75] R. Luo, Y. Men, K. Lee, W. Wang, D.R. Lorimer and B. Zhang, *On the FRB luminosity function - - II. Event rate density*, *Mon. Not. Roy. Astron. Soc.* **494** (2020) 665 [2003.04848].
- [76] J.M. Yao, R.N. Manchester and N. Wang, *A New Electron-density Model for Estimation of Pulsar and FRB Distances*, *Astrophys. J.* **835** (2017) 29 [1610.09448].
- [77] Planck Collaboration, N. Aghanim, Y. Akrami, M. Ashdown, J. Aumont, C. Baccigalupi et al., *Planck 2018 results. VI. Cosmological parameters*, *Astron. Astrophys.* **641** (2020) A6 [1807.06209].
- [78] E. Di Valentino, O. Mena, S. Pan, L. Visinelli, W. Yang, A. Melchiorri et al., *In the realm of the Hubble tension-a review of solutions*, *Classical and Quantum Gravity* **38** (2021) 153001 [2103.01183].
- [79] M. Kamionkowski and A.G. Riess, *The Hubble Tension and Early Dark Energy*, *Annual Review of Nuclear and Particle Science* **73** (2023) 153 [2211.04492].
- [80] G. Alestas, L. Kazantzidis and L. Perivolaropoulos, *H_0 tension, phantom dark energy, and cosmological parameter degeneracies*, *Phys. Rev. D* **101** (2020) 123516 [2004.08363].
- [81] S. Dahmani, A. Bouali, I. El Bojaddaini, A. Errahmani and T. Ouali, *Smoothing the H_0 tension with a phantom dynamical dark energy model*, *Physics of the Dark Universe* **42** (2023) 101266 [2301.04200].
- [82] H.K. Jassal, J.S. Bagla and T. Padmanabhan, *Observational constraints on low redshift evolution of dark energy: How consistent are different observations?*, *Phys. Rev. D* **72** (2005) 103503 [astro-ph/0506748].
- [83] U. of Cape Town, T. Carr and A. Lewis, *Uct hpc facility*, Nov., 2023. 10.5281/zenodo.10021613.